Space-charge-limited current and capacitance in double-junction diodes

A. A. Grinberg[a] and Serge Luryi
AT&T Bell Laboratories, Murray Hill, New Jersey 07974

(Received 4 August 1986; accepted for publication 22 September 1986)

An analytical theory is given for the space-charge-limited current in *n-i-n* or *p-i-p* diodes. The exact *I-V* characteristic is obtained in a parametric form. In the limit of high currents or for a large width of the intrinsic (*i*) base region the characteristics reduce to a Mott–Gurney form. In the low-current limit a linear *I-V* characteristic is obtained. The space-charge barrier presents a conceptually different case from a conventional barrier current in that the position of the barrier *moves* depending on the biasing condition. It is this motion which is responsible for the linear regime—which extends over a substantial range ($\sim 10kT/e$) of the applied voltage. The distribution of the electrostatic potential and of the quasi-Fermi level in the base, as well as the position of the potential maximum (the virtual cathode), are shown for different current levels. The differential capacitance of the double-junction diode is calculated and shown to be strongly dependent on the applied bias.

I. INTRODUCTION

Space-charge-limited (SCL) current is the main conduction mechanism in structures of the type n^+nn^+ or n^+pn^+. Following an established terminology, we shall refer to the central lightly doped region as the base. The classical realization of SCL conduction requires the absence in the base of the free carriers of the type opposite to the sign of injected carriers as well as of any fixed impurity charges. In other words, it is assumed that the density of the injected charge in the base is higher than the density of charge in the absence of the contacts. The second essential requirement of a classical SCL current is that the base thickness should be sufficiently large, so that one can neglect the influence of the second (collector) contact. (A criterion for this to be true is the inequality $\tilde{J}\tilde{L}^{3/2} \gtrsim 1$, where $\tilde{J}$ and $\tilde{L}$ are, respectively, the current density and the base thickness in dimensionless units defined below.)

Under these conditions the diode *I-V* characteristics are approximated by the Child law[1] (also called the Mott–Gurney law[2]), which can be simply derived by neglecting the diffusion component of the current and imposing the boundary condition of a vanishing electric field at the emitter contact. Corrections due to diffusion affect mainly the potential distribution near the boundaries of the base layer, without appreciably changing the *I-V* characteristics.[3]

Modern technology allows routine fabrication of *n-i-n* and *p-i-p* structures with a base (*i*) layer thicknesses of order 10^{-5} cm and less. In such diodes there is a measurable range of currents, where the above conditions of a "long" diode are violated. In this case, at low-current densities the electric field vanishes near the base center (assuming a symmetric structure) and the characteristics are quite different from the Mott–Gurney law. A study of such narrow-base structures was recently carried out by Schmidt and co-workers[4,5] on the basis of a numerical integration of the relevant differential equations. These works have clearly demonstrated the existence of a linear region in the *I-V* characteristics, which goes over into the Mott–Gurney law at higher currents. These computer studies offered no explanation for the linear regime nor described its range of validity. The authors were more interested in studying the influence of the base doping level on the characteristics of short structures than in a detailed description of the potential distribution in the base in the presence of a current.

A semianalytical approach to the problem was attempted by Van der Ziel *et al.*[6] They investigated the distribution of charge in the diode base in equilibrium, and then used qualitative reasoning—familiar from the general theory of Schottky diodes—for estimating the current. This approach, however, is valid only in the low-current limit. The essential difference between a metal-semiconductor contact and a hi-lo-hi structure is that in the former case, the barrier is fixed in space, whereas in the latter the barrier—mainly formed by a mobile charge injected into the base—moves toward the emitter contact with increasing current.

The present work develops an analytical theory of the SCL current in short structures on the assumption that the entire charge in the base (both in equilibrium and under bias) is due to mobile carriers injected into the base from the doped contact regions, i.e., in the base we neglect both the fixed charge due to any residual doping and the mobile charge thermally generated across the forbidden gap. In other words, we consider a unipolar model of an *n-i-n* or *p-i-p* structure. For the general case, the *I-V* characteristic is obtained in a parametric form. In the range of large currents or for a thick base, the characteristic goes over into the Mott–Gurney law. In the low-current limit, we derive an equation describing the linear *I-V* regime and give the range of its validity. Special attention is paid to the position of the potential maximum ("the virtual cathode") as a function of the current density. We have also considered the low-frequency differential capacitance of the diode—both at low currents, where the *I-V* characteristic is linear, and in the range of validity of the Mott–Gurney law.

Our formulation of the problem is different from that adopted in Refs. 4 and 5 mainly in the assumed model of boundary conditions. The authors of Refs. 4 and 5 had im-

[a] Also at the Department of Electrical Engineering, University of Minnesota, Minneapolis, Minnesota 55455.

 0021-8979/87/031181-09$02.40

posed a condition on the mobile charge concentration at the base edges—which was taken to be equal to the carrier concentration in the bulk of doped layers—independently of the current level. In the present work, we adopt a more realistic boundary condition corresponding to constancy of the quasi-Fermi level within the doped contact layers. This means that the concentration and the field profiles in those layers are calculated "exactly" on the assumption of a quasiequilibrium distribution, and the obtained solutions are then matched with the corresponding quantities in the base layer. Such a boundary condition was used previously in the discussion of the charge injection over planar-doped "triangular" barriers[7] as well as for calculating the *equilibrium* potential profiles in *n-i-n* diodes.[6,8]

II. GENERAL SOLUTION OF THE PROBLEM

To avoid confusion with the sign of the carrier charge, the current, and the carrier potential energy, it is convenient to consider a *p-i-p* rather than an *n-i-n* structure. We shall assume a symmetric diode, Fig. 1, with equal acceptor concentration N_A (fully ionized) in both p layers and an intrinsic (i) base of thickness L. The mobility μ and the diffusion coefficient D will be assumed field independent. It is convenient to define the dimensionless quantities: coordinate $\tilde{x}\equiv x/x_0$, potential $\tilde{\phi}\equiv\phi/\phi_0$, electric field $\tilde{E}\equiv E/E_0$, concentration of holes $\tilde{p}\equiv p/p_0$, and current density $\tilde{J}\equiv J/J_0$, with the characteristic quantities given by

$$p_0 = N_A, \tag{1a}$$

$$x_0 \equiv L_D = (\epsilon kT/4\pi e^2 N_A)^{1/2}, \tag{1b}$$

$$\phi_0 = kT/e, \tag{1c}$$

$$E_0 = kT/eL_D, \tag{1d}$$

$$J_0 = eDN_A/L_D. \tag{1e}$$

We shall assume that a negative bias is applied to the right contact layer (collector), choose the origin of x at the left (emitter) edge of the base layer, and direct the x axis toward the collector layer. With this orientation of the coordinate with respect to the field, the current will be positive.

In units (1) the Poisson and the drift-diffusion equations are of the form:

$$\frac{d\tilde{E}}{d\tilde{x}} = -\Theta(\tilde{x}) + \tilde{p}, \tag{2}$$

$$\tilde{J} = \tilde{p}\tilde{E} - \frac{d\tilde{p}}{d\tilde{x}}, \tag{3}$$

where the function $\Theta(\tilde{x})$ equals unity in the p layers and zero in the base of the diode ($0\leqslant\tilde{x}\leqslant\tilde{L}$).

In the range $0\leqslant\tilde{x}\leqslant\tilde{L}$ we can eliminate $\tilde{p}$ from Eqs. (2) and (3) and obtain a nonlinear differential equation for $\tilde{E}$:

$$\tilde{E}\frac{d\tilde{E}}{d\tilde{x}} - \frac{d^2\tilde{E}}{d\tilde{x}^2} = \tilde{J}, \tag{4}$$

of which the first integral is of the form

$$\frac{d\tilde{E}}{d\tilde{x}} - \tfrac{1}{2}\tilde{E}^2 + \tilde{J}\tilde{x} - \gamma = 0, \tag{5}$$

with γ being an integration constant. The hole concentration in the base is then defined by the equation

$$\tilde{p}(x) = \tfrac{1}{2}\tilde{E}^2 - (\tilde{J}\tilde{x} - \gamma). \tag{6}$$

It can be shown that γ must be a positive constant. Indeed, it is physically obvious that for low and moderate currents, $\tilde{J} < 1$, the potential must have a maximum within the base region (the situation when the maximum moves into the doped emitter layer or disappears there entirely, falls outside our model, since it corresponds to currents so high that one can no longer neglect the drop of the quasi-Fermi level in the doped regions). At the point of the maximum $\tilde{x} = \tilde{x}_{\max}$ one has $\tilde{E} = 0$, and Eq. (6) implies that positive concentration can be ensured only if $\gamma > \tilde{J}\tilde{x}_{\max} > 0$.

Introducing a new function

$$U\tilde{x} = \exp\left(-\frac{1}{2}\int^{\tilde{x}} \tilde{E}\,d\tilde{x}\right) \tag{7}$$

and a new independent variable

$$\xi = \tfrac{1}{2}(2/\tilde{J})^{2/3}(\tilde{J}\tilde{x} - \gamma), \tag{8}$$

reduces Eq. (5) to a linear equation:

$$\frac{d^2U}{d\xi^2} - \xi U(\xi) = 0. \tag{9}$$

The electric field in the new variables is given by

$$\tilde{E} = -(4\tilde{J})^{1/3}\frac{d\ln U(\xi)}{d\xi}, \tag{10}$$

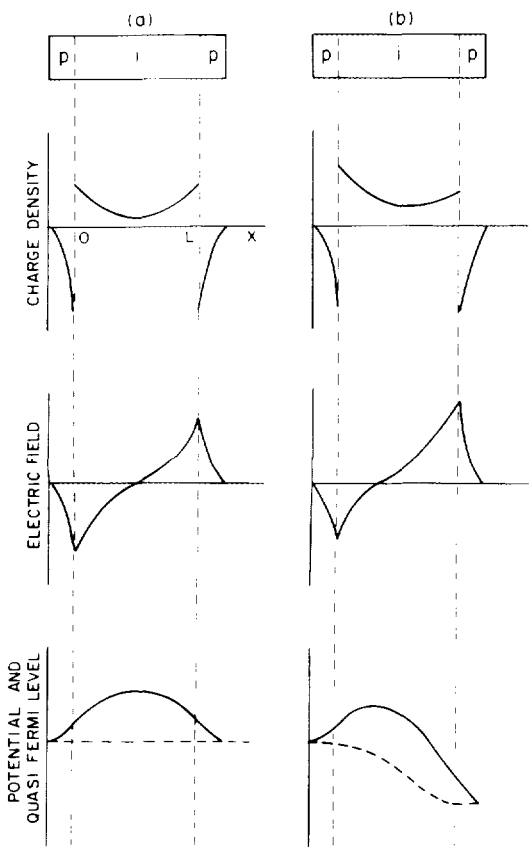

FIG. 1. Illustration of the *n-i-n* diode in equilibrium (a) and under applied bias (b). Schematically shown are profiles of the charge, the electric field, and the electrostatic potential energy. The energy diagram also shows the quasi-Fermi level (dashed line). The main approximation of this work consists in the assumption that the quasi-Fermi level is constant within the doped contact layers, resulting in the boundary conditions (5) on the electric field in the base i.

and the potential referred to its value at the emitter-base boundary by

$$\tilde{\phi}(\tilde{x}) = -\int_0^{\tilde{x}} \tilde{E}\, d\tilde{x} = 2 \ln \frac{U(\xi)}{U(\xi_0)}, \tag{11}$$

where

$$\xi_0 = -(\gamma/2)(2/\tilde{J})^{2/3}. \tag{12}$$

Equation (9) has a standard solution, given by the Bessel functions of index $\nu = 1/3$ and argument

$$z = \tfrac{2}{3}\xi^{3/2}. \tag{13}$$

Inasmuch as the variable ξ can change sign within the diode base, $\xi = 0$ is a branch point, where the argument z goes from the real to the imaginary axis. However, an inspection of Eq. (9) reveals that it has no singularities, and hence the appearance of a branch point is an artifact of the solution as given by the Bessel functions. It is, therefore, natural to determine independent solutions of (9), which would have no singularities at $\xi = 0$. Of course, these independent solutions can be expressed through the Bessel functions, but the actual expression will have a different form for $\xi < 0$ and $\xi > 0$.

Applying the usual series-expansion procedure in powers of ξ, the sought independent solutions of Eq. (9) can be written in the form

$$Y_\nu^{(1)}(\xi) = \sum_{k=0}^{\infty} \frac{\xi^{3k+1}}{3^{2k+\nu} k!\Gamma(k+1+\nu)}, \tag{14a}$$

$$Y_\nu^{(2)}(\xi) = \sum_{k=0}^{\infty} \frac{\xi^{3k}}{3^{2k-\nu} k!\Gamma(k+1-\nu)}, \tag{14b}$$

where $\nu \equiv 1/3$. The functions $Y_\nu^{(1)}$ and $Y_\nu^{(2)}$ are related as follows:

$$Y_\nu^{(1)}(\xi) = \xi Y_{-\nu}^{(2)}(\xi) \quad (\nu \equiv 1/3). \tag{15}$$

Also, from definition (14) it follows that

$$\frac{dY_\nu^{(1)}(\xi)}{d\xi} = Y_{2\nu}^{(2)}(\xi); \quad \frac{dY_\nu^{(2)}(\xi)}{d\xi} = \xi Y_{2\nu}^{(1)}(\xi). \tag{16}$$

Representations of the functions $Y_\nu^{(1)}$ and $Y_\nu^{(2)}$ through the Bessel functions are given in Appendix A. These expressions allow one to derive an asymptotic representation of the Y functions from the known representation of the Bessel functions.

All the quantities of physical interest are expressed through the function $U(\xi)$, either as a ratio of its values at two different points of the base [cf. Eq. (11)] or as its logarithmic derivative [cf. Eq. (10)]. Therefore, integration of Eq. (9) introduces only one arbitrary constant in the general physical solution. This solution can be conveniently written in the form

$$U(\xi) = \frac{\cos(\delta)\sin(\pi\nu/2)V_1(\xi) - \sin(\delta)\cos(\pi\nu/2)V_2(\xi)}{\sin(\pi\nu)}, \tag{17}$$

where δ is an integration constant, and the functions V_1 and V_2 are given by

$$V_1(\xi) = Y_\nu^{(1)}(\xi) - Y_\nu^{(2)}(\xi), \tag{18a}$$

$$V_2(\xi) = Y_\nu^{(1)}(\xi) + Y_\nu^{(2)}(\xi). \tag{18b}$$

From Eq. (10) and using (16), the electric field is expressed in the form

$$\tilde{E}(\xi) = -(4\tilde{J})^{1/3} \frac{\cos(\delta)\sin(\pi\nu/2)V_3(\xi) - \sin(\delta)\cos(\pi\nu/2)V_4(\xi)}{\cos(\delta)\sin(\pi\nu/2)V_1(\xi) - \sin(\delta)\cos(\pi\nu/2)V_2(\xi)}, \tag{19}$$

where

$$V_3(\xi) = Y_{2\nu}^{(2)}(\xi) - \xi Y_{2\nu}^{(1)}(\xi), \tag{20a}$$

$$V_4(\xi) = Y_{2\nu}^{(2)}(\xi) + \xi Y_{2\nu}^{(1)}(\xi). \tag{20b}$$

The constants γ and δ can be determined in terms of the boundary values of the electric field $\tilde{E}_0 \equiv \tilde{E}(x=0)$ and $\tilde{E}_L \equiv \tilde{E}(x=L)$. However, the practical use of Eqs. (17) and (20) is difficult because of a wide range in the variation of ξ. From the expressions of the functions $V_n(\xi)$ in terms of the Bessel functions (see Appendix A), it is evident that at large positive values of ξ the functions V_1 and V_3 are proportional to $\exp(-z)$ and the functions V_2 and V_4 are proportional to $\exp(z)$, where z is given by (13). It is therefore convenient to factor out the corresponding exponents from these functions, which would allow control of the magnitude of the individual terms in Eqs. (17) and (19). To this effect, let us introduce four new functions $V_n^*(\xi)$ of the form

$$V_{1,3}^*(\xi) = e^{z\Theta(\xi)} V_{1,3}(\xi), \tag{21a}$$

$$V_{2,4}^*(\xi) = e^{-z\Theta(\xi)} V_{2,4}(\xi), \tag{21b}$$

where $\Theta(\xi)$ is the step function. [These functions coincide with $V_n(\xi)$ for negative ξ.]

Using one of the boundary conditions, $\tilde{E}(x=L) = \tilde{E}_L$, we can eliminate the integration constant δ from Eqs. (17) and (20) (the other constant γ remaining in the definition of ξ), giving

$$U(\xi) = e^{-z\Theta(\xi)}\left(V_1^*(\xi) - AV_2^*(\xi)\exp\{-2[z_L\Theta(\xi_L) - z\Theta(\xi)]\}\right); \tag{22}$$

$$\tilde{E}(\xi) = -(4\tilde{J})^{1/3} \frac{V_3^*(\xi) - AV_4^*(\xi)\exp\{-2[z_L\Theta(\xi_L) - z\Theta(\xi)]\}}{V_1^*(\xi) - AV_2^*(\xi)\exp\{-2[z_L\Theta(\xi_L - z\Theta(\xi)]\}}, \tag{23}$$

where

$$A \equiv \frac{V_3^*(\xi_L) + V_1^*(\xi_L)[\tilde{E}_L/(4\tilde{J})^{1/3}]}{V_4^*(\xi_L) + V_2^*(\xi_L)[\tilde{E}_L/(4\tilde{J})^{1/3}]}; \quad \xi_L \equiv \xi(x=L); \quad z_L \equiv \tfrac{2}{3}\xi_L^{3/2}. \tag{24}$$

To determine the electric field at the boundaries of the base layer, we assume that the adjacent doped layers are in a quasiequilibrium state, i.e., even in the presence of a current we shall take the hole concentration in those layers in the Boltzmann form, viz., $\tilde{p} = \exp[-\tilde{\phi}(\tilde{x})]$. The Poisson equation (2) then gives

$$\tilde{E}(0) \equiv \tilde{E}_0 = -[2(\tilde{\phi}_0 + \exp(-\tilde{\phi}_0) - 1)]^{1/2}, \quad (25a)$$

$$\tilde{E}(L) \equiv \tilde{E}_L = [2(\tilde{\phi}_L + \exp(-\tilde{\phi}_L) - 1)]^{1/2}, \quad (25b)$$

where $\tilde{\phi}_0$ and $\tilde{\phi}_L$ are the potentials at points $x = 0$ and $x = L$, referred to their values in the bulk of the doped contact layers, where the electric fields vanish,

$$E(-\infty) = E(+\infty) = 0.$$

The Boltzmann approximation leading to (25) is equivalent to neglecting the drop of the quasi-Fermi levels within the doped contact layers. Validity of this approximation is conditioned on the fact that in these layers both the diffusion and the drift components of the current are much larger than the net current itself. This requirement can be expressed by the inequalities

$$\tilde{E}_0 \exp(-\tilde{\phi}_0) \gg \tilde{J}, \quad (26a)$$

$$\tilde{E}_L \exp(-\tilde{\phi}_L) \gg \tilde{J}. \quad (26b)$$

Substituting $\tilde{p}(0)$ and $\tilde{p}(L)$ in Eq. (6) and using (25), we obtain the expressions

$$\tilde{\phi}_0 = 1 - \gamma, \quad (27a)$$

$$\tilde{\phi}_L = 1 - \gamma + \tilde{J}\tilde{L}, \quad (27b)$$

from which we can express the boundary values of the field in terms of the constant γ and the current:

$$\tilde{E}_0 = -[2(\exp(\gamma - 1) - \gamma)]^{1/2}, \quad (28a)$$

$$\tilde{E}_L = \{2[\exp(\gamma - 1 - \tilde{J}\tilde{L}) - \gamma + \tilde{J}\tilde{L}]\}^{1/2}. \quad (28b)$$

Substitution of Eqs. (28) into (23) and (24) at $\xi = \xi_0$ (corresponding to $x = 0$) thus leads to a transcendental equation which determines γ. According to Eq. (11), the current-voltage characteristic is then determined by the equation

$$\tilde{V} = \tilde{\phi}_0 - \tilde{\phi}_L + 2\ln[U(\xi_L)/U(\xi_0)], \quad (29)$$

which also takes into account variations of the electrostatic potential in the doped regions.

III. THE LIMIT OF HIGH CURRENTS OR LARGE BASE THICKNESSES

When the current density is high and/or the base is thick, the diode I-V characteristic becomes close to that given by the Mott–Gurney law (MG). In a diode of a given geometry (fixed L), the characteristic asymptotically approaches MG with increasing $\tilde{J}$; at a given low-current point of the characteristic, the asymptotic approach to MG value occurs with increasing $\tilde{L}$. Formal criteria of the applicability of MG are given by the inequalities

$$\xi_L > 0 \quad \text{and} \quad z_L \gg 1. \quad (30)$$

When these inequalities are fulfilled, there is a range of z where $z_L - z \gg 1$. In this range we can neglect the terms proportional to A in Eqs. (22) and (23). Physically, this corresponds to a complete neglect of the influence of the collector contact on the field and potential distributions in the base. The function $U(\xi)$ and the field are then given by the expressions

$$U(\xi) = e^{-z\Theta(\xi)} V_1^*(\xi), \quad (31a)$$

$$\tilde{E}(\xi) = -(4\tilde{J})^{1/3} \frac{V_3(\xi)}{V_1(\xi)} = (4\tilde{J})^{1/3} \xi^{1/2} \frac{K_{2\nu}(z)}{K_\nu(z)}, \quad (31b)$$

which, in principle, describe the situation considered by Shockley and Prim.[3] The value of γ in Ref. 3 was set equal to 0, although in this approximation γ should be determined as the root of the equation

$$(4\tilde{J})^{1/3} \xi_0^{1/2} [K_{2\nu}(z_0)/K_\nu(z_0)] = \sqrt{2[\exp(\gamma - 1) - 1]}. \quad (32)$$

Figure 2 shows the dependence of the ratio $\tilde{E}(\xi)/(4\tilde{J})^{1/3}$, calculated from (31). It is evident from this figure, that the point where the electric field vanishes (the "virtual cathode") corresponds to $\xi \approx -1$. It, therefore, follows that the position of the virtual cathode in the high-current limit is approximately given by

$$\tilde{x}_{\max} = \frac{\gamma}{\tilde{J}} - \left(\frac{2}{\tilde{J}}\right)^{1/3}, \quad (33)$$

where γ is also a function of the current density $\tilde{J}$, which can be determined from (32). Plotting $\log \gamma$ vs $\log \tilde{J}$ (Fig. 3, solid line), we see that in the high-current/thick-base limit the dependence falls on a straight line, for which a good approximation is the following formula:

$$\gamma \approx 1.58\, \tilde{J}^{3/5}. \quad (34)$$

According to Eqs. (33) and (34), the virtual cathode $\tilde{x}_{\max}$ moves toward the junction as the current increases. The exact dependence $\tilde{x}_{\max}(J)$ will be discussed in Sec. V.

The MG law follows directly from Eq. (31b). Indeed, for $z_L \gg 1$, there is within the base a large region where $z \gg 1$. From the asymptotic expansion of the $K_\mu(z)$ functions we find

$$\tilde{E}(\xi) = (2\tilde{J}\tilde{x})^{1/2}. \quad (35)$$

This solution is well known to correspond to neglecting the diffusion of injected carriers. Equation (35) implies the MG

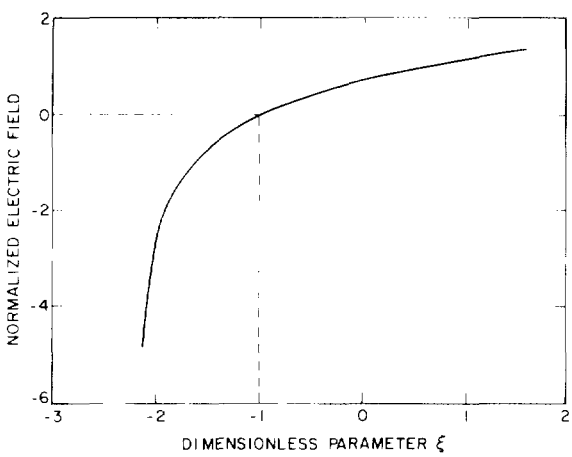

FIG. 2. Dependence of the electric field normalized to the value of the current (in the high-current limit) on the parameter ξ. Plotted is the dimensionless ratio $\tilde{E}/(4\tilde{J})^{1/3}$ calculated from Eq. (31). It is evident that position $x_{\max}$ of the virtual cathode corresponds to the value $\xi(x_{\max}) \approx -1$.

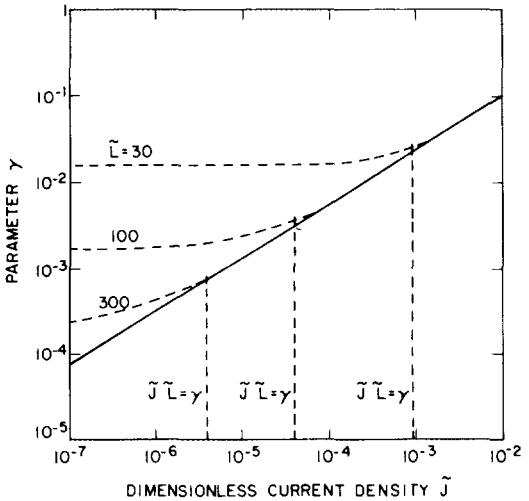

FIG. 3. Dependence of the parameter γ on the current density. Dashed lines show the exact solution calculated form Eqs. (23), (24), and (28). Solid line indicates the approximate solution in the high-current limit, calculated from Eq. (32). Vertical dashes indicate points where the parameter $\tilde{J}\tilde{L}/\gamma = 1$.

law, which in our units takes the form

$$\tilde{J} = \tfrac{9}{8}(\tilde{V}^2/\tilde{L}^3). \tag{36}$$

IV. LOW-CURRENT LIMIT

In this limit, the nature of the electric field distribution in the base is substantially different from that corresponding to the Mott–Gurney law. Accordingly, our analytical description is also qualitatively different in this range. In the limit $\tilde{J}\to 0$ the variable ξ tends to $-\infty$, and we can use the asymptotic expansions of the functions Y_ν, which follow from the relation of these functions to the Bessel functions, given in Appendix A. Using these expansions, the functions $U(\xi)$ and $\tilde{E}(\xi)$, defined by Eqs. (17) and (19), respectively, can be cast in the form

$$U(\xi) = -(-\xi)^{1/2}[S_\nu^{(1)}(z^*)\cos(\zeta) - S_\nu^{(2)}(z^*)\sin(\zeta)], \tag{37}$$

$$\tilde{E}(\xi) = -(4\tilde{J})^{1/3}(-\xi)^{1/2} \times \frac{S_{2\nu}^{(1)}(z^*)\sin(\zeta) + S_{2\nu}^{(2)}(z^*)\cos(\zeta)}{S_\nu^{(1)}(z^*)\cos(\zeta) - S_\nu^{(2)}(z^*)\sin(\zeta)}, \tag{38}$$

where

$$\zeta \equiv z^* - (\pi/4) + \delta, \quad z^* \equiv \tfrac{2}{3}(-\xi)^{3/2},$$

and the S functions are given by a series expansion (see Appendix A).

Since $z^*\to\infty$ for $\tilde{J}\to 0$, it is convenient to redefine the constant δ in such a way that the phase ζ would not contain terms diverging at $\tilde{J}\to 0$. For this purpose, let us introduce the following quantities:

$$g = \sqrt{\gamma/2}; \quad z_0 = 4g^3/3\tilde{J}; \quad \delta^* = \delta + z_0 - (\pi/4); \tag{39}$$

$$\bar{z} = z^* - z_0 = z_0\{[1 - (\tilde{x}\tilde{J}/2g^2)]^{3/2} - 1\}. \tag{40}$$

The phase ζ is then given by

$$\zeta = (\bar{z} + z_0) - (\pi/4) + [\delta^* - z_0 + (\pi/4)] = \bar{z} + \delta^*. \tag{41}$$

For $\tilde{J}\to 0$, one has $\bar{z}\to -g\tilde{x}$, and hence the phase remains finite.

From the definitions of the S functions it is easy to see that as $z^*\to\infty$, the ratio $S_\nu^{(2)}/S_\nu^{(1)}$ vanishes $\propto 1/z^*$. Restricting ourselves to the first terms in the expansions of the $S_\nu^{(1)}$ functions and to the second terms in the expansions of the $S_\nu^{(2)}$ functions, we obtain the following approximate equation:

$$U(\tilde{x}) = \left(1 - \frac{\tilde{x}\tilde{J}}{\gamma}\right)^{-1/4}\left(\cos(\bar{z} + \delta^*) + \frac{5\tilde{J}}{96g^3}\sin(\bar{z} + \delta^*)\right). \tag{42}$$

When $J\to 0$, the following relations hold to within terms of order $\pi/\tilde{L}$ (see Appendix B):

$$g\to g_0 = \frac{\pi}{\tilde{L}}\frac{1}{1+\Delta}; \quad \delta^*\to\delta_0^* = \frac{\pi}{2}\frac{1}{1+\Delta}, \tag{43}$$

where $\Delta \equiv 2^{3/2}\tilde{L}^{-1}\exp(1/2)$. [In this limit, the physical meaning of the quantity $\gamma_0 \equiv 2g_0^2$ is that it represents the hole concentration $\tilde{p}(L/2)$ in the middle of the diode (see Appendix B).] This implies the following relation:

$$\lambda \equiv \frac{\tilde{J}\tilde{x}}{2g^2} \lesssim \frac{\tilde{J}\tilde{L}^3(1+\Delta)^2}{2\pi^2}.$$

The parameter $\bar{z}$ can be written in the form

$$\bar{z} = \frac{3}{2g\tilde{x}}\frac{(1-\lambda)^{3/2} - 1}{\lambda}.$$

Thus, evaluation of the linear portion of the current-voltage characteristic reduces to expanding all the parameters in Eq. (42) to within terms linear in λ. As shown in Appendix C, if we neglect terms of order $(\pi/\tilde{L})^2$ compared to unity, then the equation determining the current-voltage characteristic is of the form

$$\tilde{J} = -\frac{4\pi^2\tilde{V}}{\tilde{L}^3(1+\Delta)^3}. \tag{44}$$

The current-voltage characteristics $\tilde{J}(\tilde{V})$, calculated from (44) for three different values of $\tilde{L}$, are shown in Fig. 4 by the dash-dotted lines. We see that for low voltages these curves practically coincide with the exact solution shown by the solid lines. Formally, Eq. (44) holds in the range given by the following inequality:

$$\frac{\tilde{J}\tilde{L}^3}{2\pi^2}(1+\Delta)^2 < 1. \tag{45}$$

Substituting (44) into (45), we get

$$\tilde{V} < (1+\Delta)/2. \tag{46}$$

Equation (46) implies that the linear range of the I-V characteristic is limited to voltages $V \lesssim kT$. However, as seen from Fig. 4, the linear range in fact extends to much higher voltages, up to $V \approx 10\,kT$. Figure 3 shows by the dashed lines the dependencies of the parameter γ on the current, calculated *on the basis of the exact solution* for three different values of $\tilde{L}$. On each of these lines we have indicated (by a vertical dash) the point where the parameter $\tilde{J}\tilde{L}/\gamma \equiv \tilde{J}\tilde{L}/2g^2$ equals unity. The corresponding points of the I-V characteristics are also marked by the vertical dashes in Fig. 4. It is clearly evident that deviation from the linearity is quite weak in an extended range beyond these points.

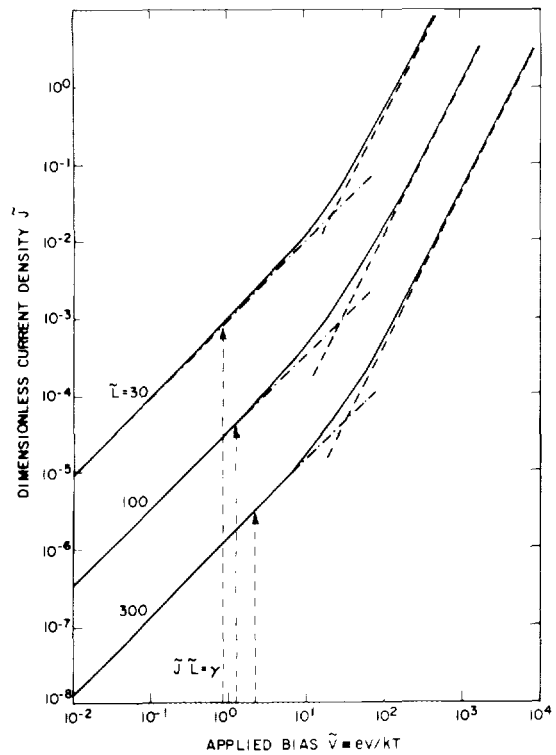

FIG. 4. Calculated current-voltage characteristics of a *p-i-p* diode. Solid lines represent the exact solution obtained from Eqs. (23)–(25) with boundary conditions (28). Dashed lines correspond to the Mott–Gurney regime (Sec. III) and dash-dotted lines describe the low-current limit (Sec. IV). Vertical dashes indicate points where the parameter $\tilde{J}\tilde{L}/\gamma = 1$, as in Fig. 3.

Equation (44) can be brought into a different form by expressing γ_0 in terms of the *equilibrium* hole concentration $\tilde{p}_0(\tilde{x})$. As shown in Appendix B, in the middle of the diode one has $\tilde{p}_0(\tilde{L}/2) = 2g_0^2$. Equation (44) thus takes the form

$$\tilde{J} = -\frac{2\tilde{p}_0(\tilde{L}/2)\tilde{V}}{\tilde{L}(1+\Delta)} \quad \text{or} \quad J = -\frac{ep_0(L/2)\mu}{1+\Delta}\frac{V}{L}, \qquad (47)$$

where μ is the low-field mobility.

The barrier in a *p-i-p* or *n-i-n* structure forms entirely due to the mobile carriers injected into the base, and any increase in the bias not only lowers the barrier electrostatically but also moves its position toward the emitter contact. The fact that the *I-V* curves show little deviation from a linear characteristic up to voltages of order $10\,kT$, indicates that carriers participating in the current do not dissipate any extra energy due to this barrier. The energy required by a hole to move over the barrier maximum is in fact supplied (through electrostatic interaction) by another hole moving away from the peak. The situation is rather similar to that corresponding to the drift of injected *minority* carriers. Indeed, when a packet of electrons injected in a *p*-type sample is drifting in an applied field, the counterflux of holes—neutralizing the electron packet—is *not* doing work against the Dember field.

V. GENERAL ANALYSIS OF THE *I-V* CHARACTERISTICS

The complete picture of the field distribution and the *I-V* characteristics can be obtained from the exact solution, described by Eqs. (23)–(25) with the boundary conditions (28). The current-voltage characteristics calculated from these equations are shown in Fig. 4 by the solid lines for three exemplary values of the base width. Figure 4 also shows the approximate solutions—corresponding to the low and high-current regimes—discussed in Secs. III and IV. As expected, in the high-current limit the characteristics asymptotically approach the Mott–Gurney curves. As to the low-current regime, it is especially noteworthy that the linear approximation (44) remains accurate in a rather large range—up to an applied bias of order $10\,kT/e$. This again supports our contention that currents over a space-charge barrier cannot be considered by analogy with the usual treatments of the charge injection over spatially fixed barriers. It is precisely due to the displacement of x_{max} with increasing current that the linear *I-V* characteristic persists to considerable biases. Figure 5 shows the potential profile in a diode of base width $\tilde{L} = 30$ for different values of the current. Dependence of the position x_{max} of the virtual cathode on the current density $\tilde{J}$ is presented in Fig. 6 for three values of the base width (for same $\tilde{L}$ as those used in Fig. 4). We see that the virtual

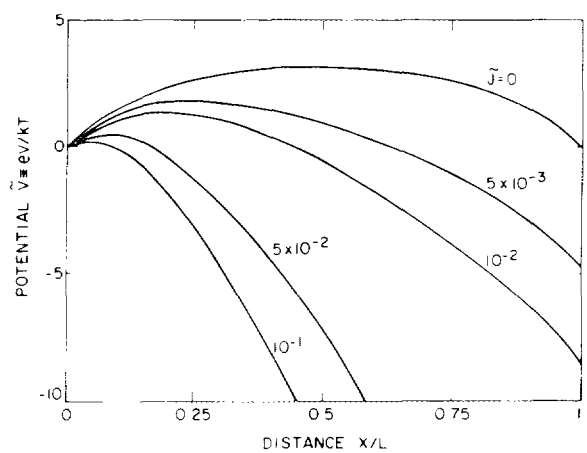

FIG. 5. Exact potential profile in a diode of base width $\tilde{L} = 30$, calculated for several values of the current density.

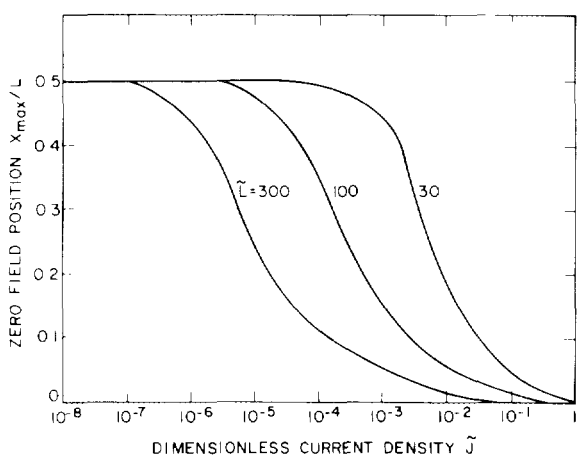

FIG. 6. Dependence of the position x_{max} of the virtual cathode on the current density, calculated for different values of the base width.

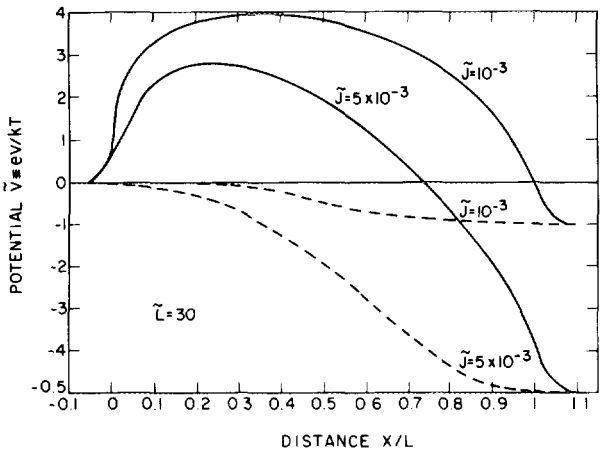

FIG. 7. Distribution of the electrostatic potential (solid lines) and of the quasi-Fermi level (dashed lines) across a double-junction diode of base width $\tilde{L}=30$ at two different current densities.

cathode approaches the emitter contact faster as the base widens.

It is instructive to consider the behavior of the quasi-Fermi level E_F, which is defined by the relation

$$\tilde{p}(x)=\exp(\tilde{E}_F-\tilde{V}).$$

Figure 7 shows the position dependencies of both $\tilde{E}_F$ and $\tilde{V}$, calculated for two different current densities in a p-i-p structure with $\tilde{L}=30$. Of course, the quasi-Fermi level is constant in the doped contacts, which is the basic approximation of our model. However, we see that it is also relatively flat in the vicinity of both boundaries in the base. At low currents, most of the variation in E_F is concentrated near the middle of the base. With an increasing current most of the drop in E_F is shifted toward the collector contact. This is as expected: on the uphill slope of the space-charge barrier the current is *a difference* of two oppositely directed—diffusion and drift—fluxes. If in some region of the diode these fluxes are large compared to the net current, then this region is close to equilibrium and hence the E_F is nearly flat. The downhill slope is always further removed from equilibrium than the uphill slope and, naturally, most of the drop in the quasi-Fermi level occurs there.

VI. CAPACITANCE OF THE DIODE

It is instructive to consider the total capacitance between the emitter and the collector electrodes in our diode. If the base were heavily doped (so that in its middle one would have quasineutrality of the total charge), then the total capacitance would be described by space-charge capacitances at the base boundaries, as is the case in a bipolar junction transistor at low injection levels. These junction capacitances in our case would be series connected. Another limiting case corresponds to a complete absence of mobile charge in the base, which would imply a total capacitance of order $\epsilon/4\pi L$. The situation is somewhat more complicated in the case under consideration since an applied voltage drops nonuniformly across the base and the total capacitance, which could be considered to be resulting from a series-connected assembly of differentially thin capacitors, can deviate rather far from the intuitive estimates based on the geometry.

This capacitance is calculated below in the limit of low frequencies, which allows us to neglect all relaxation processes associated with the carrier diffusion and drift.

Inasmuch as there is a point in the base where the electric field vanishes, the total capacitor can be regarded as a series connection of two capacitors separated by the $E=0$ plane. The total positive charge in these capacitors is given by Gauss's law:

$$Q_1=-(\epsilon E_0/4\pi),\quad Q_2=\epsilon E_L/4\pi. \tag{48}$$

The differential capacitance of the entire diode equals

$$C=\frac{\partial Q_1}{\partial V}=-\frac{\epsilon}{4\pi}\frac{\partial E_0}{\partial V}=-\frac{\epsilon}{4\pi L_D}\frac{\partial \tilde{E}_0}{\partial \tilde{V}}. \tag{49}$$

In the linear range of the I-V characteristic, the above derivative can be evaluated from Eq. (C6): $\partial\tilde{E}_0/\partial\tilde{V}=\partial\delta\tilde{E}_0/\partial\tilde{V}$, where $\delta\tilde{E}_0$ is defined in Appendix C. Using Eqs. (C6) and (44), we find

$$C=-\frac{\epsilon}{4\pi L_D}\frac{\partial\tilde{E}_0}{\partial\tilde{J}}\frac{\partial\tilde{J}}{\partial\tilde{V}}\equiv\frac{\epsilon}{4\pi L^*}, \tag{50}$$

where the second identity defines an effective width of the capacitor's gap L^*, given by

$$L^*=\frac{L^2}{L_D}\frac{(1+\Delta)^3}{2^{3/2}\pi^2\sinh(1/2)}. \tag{51}$$

The effective gap width L^* thus differs by a dimensionless factor from the geometric base width L (for large $\tilde{L}$ one has $L^*/L\approx 0.07\tilde{L}$). However, as will soon become clear, the ratio L^*/L cannot grow indefinitely with increasing L.

The time constant τ of capacitive relaxation in the linear region is, therefore, of the form

$$\tau=CR_d=C\frac{\partial V}{\partial J}=C\frac{L_D}{\sigma}\frac{\partial\tilde{V}}{\partial\tilde{J}}=\frac{\epsilon}{4\pi\sigma}\frac{\partial\tilde{E}_0}{\partial\tilde{J}}$$
$$=2^{-1/2}\sinh(1/2)\tau_\sigma\frac{L}{L_D}, \tag{52}$$

where $\tau_\sigma\equiv\epsilon/4\pi\sigma$ and $\sigma\equiv e\mu N_A$. It should be noted (cf. Appendix C) that Eqs. (50)–(52) are valid provided $\tilde{L}\gg 1$ and their accuracy holds within terms of order $1/\tilde{L}$.

In the high-current regime, where the Mott–Gurney law holds, the diode capacitance will be entirely determined by the variation of charge Q_2 with an applied voltage V, since the voltage drop V_1 in the "first capacitor" can be expected to be small compared to V. We can, therefore, assume that $\partial Q_2/\partial V_2\approx\partial Q_2/\partial V\approx\partial Q/\partial V$, where Q is the total charge in the base. Taking $\tilde{E}_L=(2\tilde{J}\tilde{L})^{1/2}$ [cf. Eq. (35)] and using (36) we obtain

$$C=\frac{\epsilon}{4\pi}\frac{\partial E_L}{\partial V}=\frac{\epsilon}{4\pi L_D}\frac{\partial\tilde{E}_L}{\partial\tilde{V}}=\frac{3\epsilon}{8\pi L} \tag{53}$$

and

$$\tau=\tau_\sigma\frac{\partial\tilde{E}_L}{\partial\tilde{J}}=\tau_\sigma\left(\frac{\tilde{L}}{2\tilde{J}}\right)^{1/2}=\left(\frac{\epsilon}{8\pi\mu J}\right)^{1/2}. \tag{54}$$

Comparing Eqs. (51) and (53), it is evident that at low currents, the capacitance decreases proportionally to the inverse square of the base width. As the current increases, the

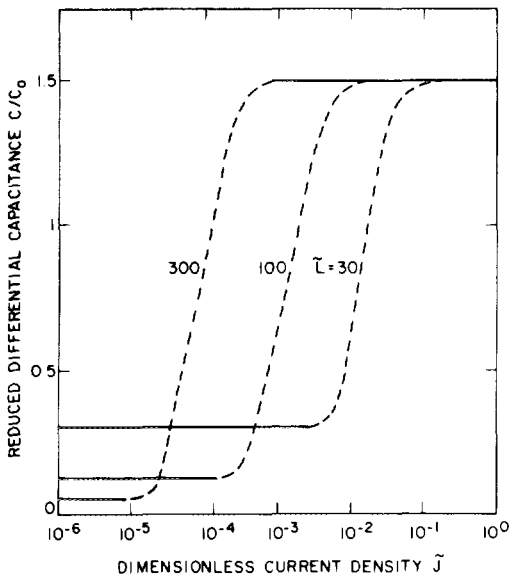

FIG. 8. Dependence of the differential capacitance of the diode on the current density $\tilde{J}$, calculated from Eqs. (50) and (53). The capacitance is expressed in units of the geometric capacitance $C_0 \equiv \epsilon/4\pi L$. Dashed lines represent an interpolation between the calculated regimes of the low and the high currents.

quadratic dependence on L weakens, and in the range of the validity of the MG law the dependence becomes inverse-linear. In that range the effective base width equals $L^* = 2L/3$.

Figure 8 shows the current dependence of the differential capacitance (in units of the "geometric" capacitance $C_0 \equiv \epsilon/4\pi L$ per unit area) calculated from Eqs. (50) and (53), which are valid, respectively, in the low- and high-current regime. Ranges of the validity of these equations were determined from Fig. 4. In the intermediate range we have adopted a simple interpolation, indicated in Fig. 8 by the dashed lines. A somewhat surprising result, following from Eq. (50), is that in the linear portion of the I-V characteristics the capacitance decreases quadratically with the base width L. This behavior is mainly a consequence of the sharp rise ($\propto L^3$) of the diode resistance evident from Eq. (44). It should be noted, however, that by increasing L at a fixed current density we must necessarily enter the high-current regime, since the low-current range shrinks as L^{-3} [cf. the inequality (45)].

APPENDIX A: Y FUNCTIONS AND BESSEL FUNCTIONS; ASYMPTOTIC EXPANSIONS

Relation of the functions $Y_\nu^{(1)}, Y_\nu^{(2)} Y_{2\nu}^{(1)}$, and $Y_{2\nu}^{(2)}$ ($\nu \equiv 1/3$) to the Bessel functions can be established by comparing their defining power series. These relations are given by the following expressions.

For $\xi \geqslant 0$:

$$Y_\nu^{(1)}(\xi) = \xi^{1/2} I_\nu(z), \tag{A1a}$$

$$Y_{2\nu}^{(1)}(\xi) = I_{2\nu}(z), \tag{A1b}$$

$$Y_\nu^{(2)}(\xi) = \xi^{1/2} I_{-\nu}(z), \tag{A1c}$$

$$Y_{2\nu}^{(2)}(\xi) = \xi I_{-2\nu}(z), \tag{A1d}$$

For $\xi \leqslant 0$:

$$Y_\nu^{(1)}(\xi) = -(-\xi)^{1/2} J_\nu(z^*), \tag{A2a}$$

$$Y_{2\nu}^{(1)}(\xi) = -J_{2\nu}(z^*), \tag{A2b}$$

$$Y_\nu^{(2)}(\xi) = (-\xi)^{1/2} J_{-2\nu}(z^*), \tag{A2c}$$

$$Y_{2\nu}^{(2)}(\xi) = -\xi J_{-2\nu}(z^*), \tag{A2d}$$

where

$$\nu \equiv \tfrac{1}{3}, \quad z \equiv \tfrac{2}{3}\xi^{3/2}, \quad \text{and} \quad z^* = \tfrac{2}{3}(-\xi)^{3/2}.$$

Here and below, I_μ, J_μ, K_μ are the Bessel functions (cf. Ref. 9, p. 951) of a real (J) or imaginary (I,K) argument.

The combinations of Y functions introduced in Eqs. (18) and (20) are expressed in terms of the Bessel functions as follows.

For $\xi \geqslant 0$:

$$V_1(\xi) = -[2\sin(\pi\nu)/\pi]\xi^{1/2} K_\nu(z), \tag{A3a}$$

$$V_2(\xi) = \xi^{1/2}[I_\nu(z) + I_{-\nu}(z)], \tag{A3b}$$

$$V_3(\xi) = [2\sin(\pi\nu)/\pi]\xi K_{2\nu}(z), \tag{A3c}$$

$$V_4(\xi) = \xi[I_{2\nu}(z) + I_{-2\nu}(z)]. \tag{A3d}$$

For $\xi \leqslant 0$:

$$V_1(\xi) = -(-\xi)^{1/2}[J_\nu(z^*) + J_{-\nu}(z^*)], \tag{A4a}$$

$$V_2(\xi) = -(-\xi)^{1/2}[J_\nu(z^*) - J_{-\nu}(z^*)], \tag{A4b}$$

$$V_3(\xi) = \xi[J_{2\nu}(z^*) - J_{-2\nu}(z^*)], \tag{A4c}$$

$$V_4(\xi) = -\xi[J_{2\nu}(z^*) + J_{-2\nu}(z^*)]. \tag{A4d}$$

For our purposes, it is convenient to use the following asymptotic representation of the Bessel function $J_\mu(z^*)$ (arbitrary μ) in the limit of large z^* (cf. Ref. 9, p. 961):

$$J_\mu(z^*) = S_\mu^{(1)} \cos\left(z^* - \frac{\pi\mu}{4} - \frac{\pi}{4}\right) - S_\mu^{(2)} \sin\left(z^* - \frac{\pi\mu}{4} - \frac{\pi}{4}\right), \tag{A5}$$

where

$$S_\mu^{(1)}(\xi) = \left(\frac{2}{\pi z^*}\right)^{1/2} \sum_{k=0}^{\infty} (-)^k f(z^*, 2k), \tag{A6a}$$

$$S_\mu^{(2)}(\xi) = \left(\frac{2}{\pi z^*}\right)^{1/2} \sum_{k=0}^{\infty} (-)^k f(z^*, 2k+1), \tag{A6b}$$

and the functions $f(z^*,k)$ are defined by the recurrence relations

$$f(z^*,0) = 1; \quad f(z^*,k) = f(z^*,k-1)\frac{\mu^2 - (k-\frac{1}{2})^2}{2kz^*}. \tag{A7}$$

APPENDIX B: EQUILIBRIUM PROPERTIES OF A DOUBLE-JUNCTION STRUCTURE

For $J = 0$, Eq. (5) can be integrated, giving

$$\tilde{E} = -2g_0 \tan(\delta_0 - g_0\tilde{x}), \tag{B1}$$

where $g_0 \equiv \sqrt{\gamma_0/2}$ and the subscript "0" designates quantities corresponding to the equilibrium situation. Since, for a symmetric diode, the field must vanish exactly in the middle, one has $\delta_0 = g_0\tilde{L}/2$, whence[10]

$$\tilde{E} = -2g_0 \tan[g_0(\tilde{L}/2 - \tilde{x})]. \tag{B2}$$

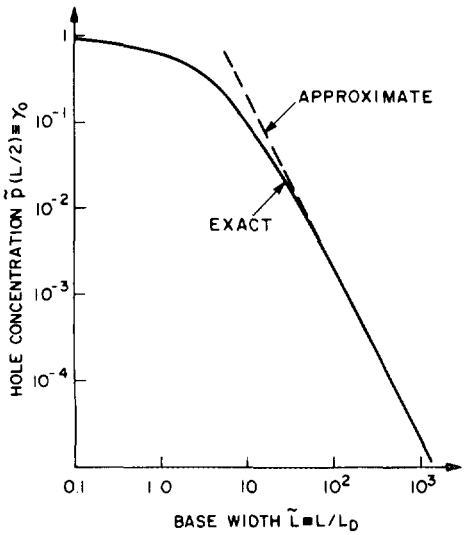

FIG. 9. Dependence of the parameter $\gamma_0 \equiv g_0^2$ on the base width. The physical meaning of γ_0 is that it equals the dimensionless hole concentration in the middle of the diode in equilibrium, i.e., $\gamma_0 = p(L/2)/N_A$. Solid line represents the exact dependence calculated from Eq. (B5), and the approximation (B6), valid for $\tilde{L} \gg 1$, is shown by the dashed line.

Differentiating (B2), one finds the hole concentration, which in the middle of the diode is given by

$$\tilde{p}_0\left(\frac{L}{2}\right) = \left(\frac{d\tilde{E}}{d\tilde{x}}\right)_{x=L/2} = 2g_0^2 \equiv \gamma_0. \tag{B3}$$

Parameter g_0 is determined from the boundary condition (28),

$$-\{2[\exp(\gamma_0 - 1) - \gamma_0]\}^{1/2} = -2g_0 \tan(g_0\tilde{L}/2), \tag{B4}$$

which can be rewritten in the form

$$\cos(g_0\tilde{L}/2) = \sqrt{2}g_0 \exp(\tfrac{1}{2} - g_0^2). \tag{B5}$$

The dependence of the equilibrium midbase hole concentration $\tilde{p}_0(L/2) = 2g_0^2$ on the base width L calculated from Eq. (B5) is shown in Fig. 9. For $\tilde{L} \gg 1$, one has $g_0 \ll 1$ and to within terms linear in g_0, one has

$$g_0\tilde{L}/2 \to \pi/2 - \sqrt{2}g_0 \exp(1/2),$$

whence we obtain Eq. (43). Note that in this limit the midbase hole concentration is independent of N_A:

$$p(L/2) \approx 2\pi^2 \epsilon kT/e^2L^2. \tag{B6}$$

Of course, this solution is valid only provided $p \gg p_i$, where p_i is the intrinsic (thermal) hole concentration in the semiconductor under consideration.

APPENDIX C: DERIVATION OF EQ. (44)

To within terms linear in the parameter

$$\lambda \equiv \tilde{J}\tilde{x}/2g_0^2,$$

the function $U(\tilde{x})$ can be written in the form

$$U(\tilde{x}) = [1 + (\tilde{J}\tilde{x}/8g_0^2)]\cos(\bar{z} + \delta^*), \tag{C1}$$

where δ^* has been redefined ($\delta^* \to \delta^* - 5\tilde{J}/96g_0^3$). To within the same accuracy, one has $\bar{z} = -g\tilde{x} + \tilde{J}\tilde{x}^2/8g_0$. Setting $\delta^* = \delta_0^* + \delta_1$ and $g = g_0 + g_1$, where g_1 and δ_1 are the variations linear in current of the respective quantities, we find that the variation of the function $U(\tilde{x})$ is given by

$$\delta U(\tilde{x}) = U_0(\tilde{x})\left[\frac{\tilde{J}\tilde{x}}{8g_0^2} + \left(g_1\tilde{x} - \delta_1 - \frac{\tilde{J}\tilde{x}^2}{8g_0}\right) \times \tan[g_0(\tilde{L}/2 - \tilde{x})]\right]. \tag{C2}$$

According to definition (7), the corresponding variation in the electric field equals

$$\delta\tilde{E} = -2\frac{\partial}{\partial\tilde{x}}\left(\frac{\delta U(\tilde{x})}{U_0(\tilde{x})}\right).$$

Equating the variations of the field at the points $x = 0$ and $x = L$ to the corresponding variations in $\tilde{E}_0$ and $\tilde{E}_L$, which, according to Eqs. (28) and (B2), are given by

$$\delta\tilde{E}(0) = \delta\tilde{E}_0 = \frac{2(1-\alpha)g_1}{\tan(g_0\tilde{L}/2)};$$

$$\delta\tilde{E}(L) = \delta\tilde{E}_L = -\frac{2(1-\alpha)}{\tan(g_0\tilde{L}/2)}\left(g_1 - \frac{\tilde{J}\tilde{L}}{4g_0}\right), \tag{C3}$$

respectively, we obtain a system of two equations which determine g_1 and δ_1. In Eqs. (C3) and below α denotes $\exp(2g_0^2 - 1)$. If we neglect terms of order g_0^2 compared to unity, and take into account the identity $\tan^2(g_0\tilde{L}/2) = (\alpha/2g_0^2) - 1$, then system (C3) yields

$$g_1 = \tilde{J}\tilde{L}/8g_0, \tag{C4}$$

$$\delta_1 = -\frac{\tilde{J}}{4g_0\alpha}\left(1 + \frac{\alpha\tilde{L}}{2g_0[(\alpha/2g_0^2) - 1]^{1/2}}\right). \tag{C5}$$

Substituting (C4) into (C3), we obtain

$$\delta\tilde{E}_0 = 2^{-1/2}\sinh(1/2)\tilde{J}\tilde{L}; \quad \delta\tilde{E}_L = \delta\tilde{E}_0. \tag{C6}$$

According to Eqs. (29) and (27), the applied potential difference is given by

$$\tilde{V} = -\tilde{J}\tilde{L} + 2\frac{\delta U(L) - \delta U(0)}{U_0}. \tag{C7}$$

Using Eqs. (C2), (C4), and (C5), we thus obtain

$$\tilde{V} = -\tilde{J}\tilde{L}\{1 + [(1+\Delta)/4g_0^2]\}, \tag{C8}$$

which leads to Eq. (44) if one neglects the potential drop ($\tilde{J}\tilde{L}$) in p-doped layers—which is small compared to the drop in the base by a factor $4g_0^2$. All equations in Appendix C are valid to within terms linear in the current density $\tilde{J}$, and Eqs. (C4)–(C8), moreover, to within terms linear in $1/\tilde{L}$.

[1] C. D. Child, Phys. Rev. **32**, 493 (1911).
[2] N. F. Mott and R. W. Gurney, *Electronic Processes in Ionic Crystals*, 2nd edition (Oxford University Press, Oxford, 1948).
[3] W. Shockley and R. C. Prim, Phys. Rev. **90**, 753 (1953).
[4] P. E. Schmidt and H. K. Henish, Solid State Electron. **25**, 1129 (1982).
[5] P. E. Schmidt, M. Octavio, and P. D. Esqueda, IEEE Electron Device Lett. **EDL-2**, 205 (1981).
[6] A. Van der Ziel, M. Shur, K. Lee, T. Chen, and K. Amberiadis, IEEE Trans. Electron Devices **ED-30**, 128 (1983).
[7] R. F. Kazarinov and S. Luryi, Appl. Phys. Lett. **38**, 810 (1981).
[8] S. Luryi and S. M. Sze, in *Silicon Molecular Beam Epitaxy*, edited by E. Kasper and J. C. Bean, CRC Uniscience (CRC, Boca Raton, FL, 1986).
[9] I. S. Gradshteyn and I. M. Ryzhik, *Table of Integrals, Series, and Products*, corrected and enlarged edition (Academic, New York, 1980).

[10] This solution also follows from our general solution in the low-current limit, considered in Sec. IV. Indeed, in the limit $\tilde{J} \to 0$ one has $\bar{z} \to -g\tilde{x}$. Equation (B2) then immediately follows from Eq. (42) and definition (7), viz., $\tilde{E} \equiv -2\partial(\ln U)/\partial\tilde{x}$.